Bridging Freidlin-Wentzell large deviations theory and stochastic thermodynamics

Davide Santolin [1], Nahuel Freitas [2], Massimiliano Esposito [3] and Gianmaria Falasco [1]
[1]*Department of Physics and Astronomy, University of Padova, Via Marzolo 8, I-35131 Padova, Italy*
[2]*Departamento de Física, FCEyN, UBA, Pabellón 1, Ciudad Universitaria, 1428 Buenos Aires, Argentina*
[3]*Complex Systems and Statistical Mechanics, Department of Physics and Materials Science, University of Luxembourg, 30 Avenue des Hauts-Fourneaux, L-4362 Esch-sur-Alzette, Luxembourg*

(Received 11 September 2024; revised 3 January 2025; accepted 7 January 2025; published 4 February 2025)

For overdamped Langevin systems subjected to weak thermal noise and nonconservative forces, we establish a connection between Freidlin-Wentzell large deviations theory and stochastic thermodynamics. First, we derive a series expansion of the quasipotential around the detailed-balance solution, that is, the system's free energy, and identify the conditions for the linear response regime to hold, even far from equilibrium. Second, we prove that the escape rate from dissipative fixed points of the macroscopic dynamics is bounded by the entropy production of trajectories that relax into and escape from the attractors. These results provide the foundation to study the nonequilibrium thermodynamics of dissipative metastable states.

DOI: 10.1103/PhysRevE.111.024106

I. INTRODUCTION

Metastability is a widespread phenomenon observed in natural systems spanning from climate science [1], chemistry, and biology [2], to man-made technological devices, like electronic bit-storage elements [3]. Heuristically, metastable states are only transiently stable, as they relax to the actual stable state by (e.g., thermal) fluctuations over exponentially long times.

For systems that enjoy detailed-balance dynamics, meaning those that experience only conservative forces and thermal noise, metastable states are local free-energy minima separated by barriers (high enough with respect to thermal energy) from their stable thermodynamic equilibrium. Diamond and supercooled water are two standard examples whose corresponding equilibria (graphene and ice) can be reached only through nucleation. The most suitable setups used to study this phenomenon are nonlinear systems described by overdamped Langevin dynamics in the limit of weak noise when, for instance, the temperature is low. The rarity of jumps among metastable states is then caused by the feeble effect of the thermal noise acting on the system. Within this framework, the description of metastable states for detailed-balance systems was derived in the early 20th century by Eyring [4] and Kramers [5], following the original ideas of Arrhenius [6], to link the lifetime of these states to the system energetics. In fact, for equilibrium systems where metastable states are (free) energy minima, the exit time τ, that is, the inverse of the escape rate r, depends exponentially on the barrier height ΔE enclosing a minimum over the thermal energy $k_B T$,

$$\tau_{\mathrm{eq}} = r_{\mathrm{eq}}^{-1} \asymp \exp\left(\frac{\Delta E}{k_B T}\right). \tag{1}$$

This result holds in the weak noise limit, that is, $\Delta E \gg k_B T$, and today is best understood within the framework of large deviations theory. The subexponential prefactor that sets the overall timescale is given by the Eyring-Kramers formula [7].

For systems that are subject to nonconservative forces, thus continuously producing entropy, one can no longer rely on the free-energy concept to describe metastable states through their minima and barriers. The most suitable definition of metastability is of pure dynamical nature: metastable Markovian systems are characterized by disparate characteristic times, as expressed by the spectrum of their stochastic generator, separated by diverging gaps.

For the case of dissipative systems subjected to a weak noise, Freidlin and Wentzell [8] developed a theory in which the exponential exit time from nonequilibrium metastable states is reminiscent of Eq. (1), but the role of the energy is played by the *quasipotential* I^{ss} [9]:

$$\tau = r^{-1} \asymp \exp\left(\frac{\Delta I^{\mathrm{ss}}}{\varepsilon}\right). \tag{2}$$

The quasipotential is defined within large deviations theory [10], when probabilities can be reasonably described by a Wentzel-Kramers-Brillouin ansatz in some weak noise limit. For systems described by Langevin dynamics with coordinates x, we have $p(x,t) \asymp \exp(-I(x,t)/\varepsilon)$, where $I(x,t)$ is the rate function associated with the system state x, and $\varepsilon \to 0^+$ is a small bookkeeping parameter that measures the noise intensity. Its stationary limit $I^{\mathrm{ss}}(x) = \lim_{t\to\infty} I(x,t)$ behaves like a potential function for the nonequilibrium dynamics, from which the name quasipotential derives [11]. Indeed, it is a Lyapunov function for the noiseless dynamics obtained by setting $\varepsilon = 0$, and determines the lifetime of attractors through Eq. (2). In general, the quasipotential I^{ss} is not known *a priori*, reducing to the scaled system energy $E/k_B T$ only for detailed-balance dynamics. For dissipative systems, I^{ss} is hard to evaluate analytically by solving the small-noise expansion of the Fokker-Planck equation [12,13] and requires dedicated numerical techniques to be extracted from simulations [14,15]. With no access to the quasipotential, Eq. (2) is far from being insightful.

In this paper, we address the problem of metastability for thermodynamic systems following non-detailed-balance dynamics [16], which can be described by overdamped diffusive processes. Moreover, we restrict ourselves to autonomous dynamics. For this class of systems, ubiquitous in, for example, soft matter physics, we provide a link between Freidlin-Wentzell theory and the nonequilibrium thermodynamics of relaxation within and escape from isolated attractors. First, we derive an iterative expansion for the quasipotential in terms of the driving force breaking detailed balance. This expansion can be readily implemented numerically, as it exploits the deterministic equilibrium relaxation only. Second, we show that the nonequilibrium escape rate r is bounded by thermodynamics. This can be useful when the exact expression for the escape rates is unavailable. The upper bound on $\ln r$ is proven to be the dissipation along the most likely escape trajectory, called *instanton*, while the lower bound is given by minus the dissipation along the most likely relaxation trajectory. These two bounds, previously derived for Markov jump processes admitting a macroscopic limit [17,18], are here extended to diffusion processes using a representation of path probabilities in terms of physical coordinates only and the orthogonal decomposition of the drift field [19,20]. The bounds saturate for detailed-balance dynamics and close to it, where relaxation and escape trajectories are mapped onto each other via time reversal.

The paper is structured as follows: in Sec. II the basic setup is provided, defining the stochastic process treated and setting the notation. In Sec. III we briefly recapitulate the stochastic thermodynamics [21–25] of overdamped Langevin systems at the level of average quantities. In Sec. IV, we derive the associated weak-noise limit using the large deviations approach. The emergent second law, previously obtained for Markov jump processes [17], is shown to hold for overdamped Langevin dynamics as well. In Sec. V we derive the nonequilibrium expansion for the quasipotential and show that the emergent second law is saturated at first order (i.e., linear response regime). In Sec. VI we introduce the orthogonal decomposition of the drift vector field. We also show that the linear response approximation of the rate function holds in the nonlinear regime when some geometric conditions are met. Sec. VII is devoted to the derivation of the thermodynamic bounds on escape rates, which are exemplified in Sec. VIII for a two-dimensional system consisting of a Brownian particle trapped in a double-well potential under the effect of a shear flow. Finally, in Sec. IX we conclude with a remark on subleading corrections to the rate function.

II. OVERDAMPED DIFFUSION PROCESSES

We consider a stochastic process described by a time-dependent probability distribution $P(\boldsymbol{x})$ over $\boldsymbol{x} \in \mathbb{R}^N$. Its evolution is given by the Fokker-Planck equation

$$\partial_t P(\boldsymbol{x}) = -\partial_n J_n(\boldsymbol{x}), \tag{3}$$

where $\partial_n \equiv \partial_{x_n}$. Repeated indices are summed over, and the current J_n is given by

$$J_n(\boldsymbol{x}) = \mu_n(\boldsymbol{x})P(\boldsymbol{x}) - D_{nm}(\boldsymbol{x})\partial_m P(\boldsymbol{x}). \tag{4}$$

Here, $\mu_n(\boldsymbol{x})$ is a drift vector and $D_{nm}(\boldsymbol{x})$ a positive-definite diffusion matrix. Both are time-independent, as we restrict ourselves to autonomous dynamics. The time dependence of $P(\boldsymbol{x})$ and $J_n(\boldsymbol{x})$ will not be written explicitly to ease notation. We assume there exists a unique steady state $P^{\rm ss}(\boldsymbol{x})$, with the corresponding current $J_n^{\rm ss}(\boldsymbol{x})$ satisfying

$$0 = \partial_n J_n^{\rm ss}(\boldsymbol{x}). \tag{5}$$

Equilibrium states are a special kind of steady state for which $J_n^{\rm ss}(\boldsymbol{x}) = 0$ for all n and $\boldsymbol{x}$. They exist if and only if the drift $\mu_n(\boldsymbol{x})$ derives from a gradient, that is, when $\mu_n(\boldsymbol{x}) = -D_{nm}(\boldsymbol{x})\partial_m\Phi(\boldsymbol{x})$ for some sufficiently confining state function $\Phi(\boldsymbol{x})$. In that case, the dynamics are said to be detailed-balanced, and the steady-state distribution is $P^{\rm eq}(\boldsymbol{x}) = e^{-\Phi(\boldsymbol{x})}/Z^{\rm eq}$, with $Z^{\rm eq} = \int d\boldsymbol{x} e^{-\Phi(\boldsymbol{x})}$. For systems in contact with a single thermal bath and subjected to conservative forces, the state function $\Phi(\boldsymbol{x})$ is given by $\Phi(\boldsymbol{x}) = E(\boldsymbol{x})/(k_B T)$ in terms of the energy $E(\boldsymbol{x})$ of state $\boldsymbol{x}$ and the thermal energy of the bath $k_B T$. In the following, we consider $k_B T = 1$ whenever we make reference to the thermodynamic interpretation. In general, we write the drift as

$$\mu_n(\boldsymbol{x}) = -D_{nm}(\boldsymbol{x})\partial_m\Phi(\boldsymbol{x}) + f_n(\boldsymbol{x}), \tag{6}$$

where $\Phi(\boldsymbol{x})$ is the thermodynamic potential and $f_n(\boldsymbol{x})$ is a generalized force, which might or might not derive from the gradient of a state function. If $f_n = -D_{nm}\partial_m\Psi(\boldsymbol{x})$, then the system will relax to a new equilibrium state associated with distribution $\tilde{P}^{\rm eq}(\boldsymbol{x}) \propto {\rm e}^{-(\Phi(\boldsymbol{x})+\Psi(\boldsymbol{x}))}$. Otherwise, the system will reach a nonequilibrium steady state with persistent currents $J_n^{\rm ss}(\boldsymbol{x}) \neq 0$. An additional decomposition of the drift field is considered in Sec. VI.

We note that the Fokker-Planck equation can be alternatively written as

$$\partial_t \mathcal{I}(\boldsymbol{x}) = \partial_n j_n(\boldsymbol{x}) - \partial_n \mathcal{I}(\boldsymbol{x}) j_n(\boldsymbol{x}) \tag{7}$$

in terms of the self-information or surprisal

$$\mathcal{I}(\boldsymbol{x}) = -\ln(P(\boldsymbol{x})), \tag{8}$$

and the reduced currents or probability velocities

$$j_n(\boldsymbol{x}) \equiv J_n(\boldsymbol{x})/P(\boldsymbol{x}) = \mu_n(\boldsymbol{x}) + D_{nm}(\boldsymbol{x})\,\partial_m\mathcal{I}(\boldsymbol{x}). \tag{9}$$

III. AVERAGE THERMODYNAMICS

Following stochastic thermodynamics [21,22], we derive the first and second laws of thermodynamics in this setting, focusing on average quantities. We note that, for a system in contact with a single thermal reservoir, the thermodynamic terminology is justified. However, for general diffusive processes, this terminology has no relation to thermodynamics and only serves as a convenient guide to interpret our results.

A. First Law

We first consider the expectation value of the potential $\langle\Phi\rangle = \int d\boldsymbol{x}\,\Phi(x)P(\boldsymbol{x})$. Using the drift in Eq. (6), its time derivative can be written in terms of two contributions

$$d_t\langle\Phi\rangle = \langle\dot{Q}\rangle + \langle\dot{W}\rangle\,. \tag{10}$$

The heat rate (energy exchanged with the reservoir) reads

$$\langle \dot{Q} \rangle = -\int d\boldsymbol{x}\; j_n(\boldsymbol{x}) D^{-1}_{nm}(\boldsymbol{x}) \mu_m(\boldsymbol{x})\, P(\boldsymbol{x}) \equiv -\langle j D^{-1} \mu \rangle \quad (11)$$

and the work rate [energy exchanged with the external force $f_n(\boldsymbol{x})$]

$$\langle \dot{W} \rangle = \int d\boldsymbol{x}\; j_n(\boldsymbol{x}) D^{-1}_{nm}(\boldsymbol{x}) f_m(\boldsymbol{x})\, P(\boldsymbol{x}) \equiv \langle j D^{-1} f \rangle \,. \quad (12)$$

B. Second Law

We now consider the Shannon entropy $S = -\int d\boldsymbol{x} P(\boldsymbol{x}) \ln(P(\boldsymbol{x}))$. Using Eq. (9), its time derivative can be written as

$$d_t S = \langle j D^{-1} j \rangle - \langle j D^{-1} \mu \rangle, \quad (13)$$

from which we obtain the usual expression for the second law of thermodynamics

$$\langle \dot{\Sigma} \rangle = d_t S - \langle \dot{Q} \rangle = \langle j D^{-1} j \rangle \geqslant 0. \quad (14)$$

Since we are considering unit temperature, $-\langle \dot{Q} \rangle$ is the rate of entropy change in the thermal environment, and therefore $\langle \dot{\Sigma} \rangle$ is the mean total entropy production rate which, according to the previous expression, is manifestly positive and vanishes at equilibrium.

The second law can also be understood in terms of a nonequilibrium free energy, that is, defined as the relative entropy between the instantaneous distribution and the equilibrium one:

$$\begin{aligned} \mathcal{F} &= \int d\boldsymbol{x}\, P(\boldsymbol{x}) \ln(P(\boldsymbol{x})/P^{\rm eq}(\boldsymbol{x})) \\ &= \langle \Phi \rangle - S + \ln(Z^{\rm eq}). \end{aligned} \quad (15)$$

Then, Eq. (14) can be rewritten as

$$\langle \dot{\Sigma} \rangle = \langle \dot{W} \rangle - d_t \mathcal{F} \geqslant 0. \quad (16)$$

C. Adiabatic and nonadiabatic decomposition

In analogy with the nonequilibrium free energy in Eq. (15), we can define the relative entropy between the instantaneous distribution and the steady-state one as

$$\mathcal{G} \equiv \int d\boldsymbol{x}\, P(\boldsymbol{x}) \ln(P(\boldsymbol{x})/P^{\rm ss}(\boldsymbol{x})), \quad (17)$$

and compute its time derivative. Using Eq. (9), we find

$$\langle \dot{\Sigma} \rangle = \langle \dot{\Sigma}_{\rm a} \rangle + \langle \dot{\Sigma}_{\rm na} \rangle, \quad (18)$$

where

$$\langle \dot{\Sigma}_{\rm a} \rangle = \langle j D^{-1} j^{\rm ss} \rangle, \quad \langle \dot{\Sigma}_{\rm na} \rangle = -d_t \mathcal{G} = \langle j D^{-1} (j - j^{\rm ss}) \rangle \quad (19)$$

are the adiabatic and nonadiabatic contributions to the entropy production [26]. An important property of $\langle \dot{\Sigma}_{\rm a} \rangle$ and $\langle \dot{\Sigma}_{\rm na} \rangle$ is that they are always positive or zero. To see that, we first note that

$$\begin{aligned} \langle j^{\rm ss} D^{-1} (j - j^{\rm ss}) \rangle &= \int d\boldsymbol{x}\, J^{\rm ss}_n(\boldsymbol{x})\, \partial_n \ln\left(\frac{P^{\rm ss}(\boldsymbol{x})}{P(\boldsymbol{x})}\right) \frac{P(\boldsymbol{x})}{P^{\rm ss}(\boldsymbol{x})} \\ &= -\int d\boldsymbol{x}\, J^{\rm ss}_n(\boldsymbol{x})\, \partial_n \left(\frac{P(\boldsymbol{x})}{P^{\rm ss}(\boldsymbol{x})}\right) = 0, \end{aligned} \quad (20)$$

where the last equality is obtained by integrating parts and using that $\partial_n J^{\rm ss}_n(\boldsymbol{x}) = 0$. Then, it follows that

$$\langle \dot{\Sigma}_{\rm a} \rangle = \langle j^{\rm ss} D^{-1} j^{\rm ss} \rangle \geqslant 0 \quad (21)$$

and

$$\langle \dot{\Sigma}_{\rm na} \rangle = -d_t \mathcal{G} = \langle (j - j^{\rm ss}) D^{-1} (j - j^{\rm ss}) \rangle \geqslant 0 \,, \quad (22)$$

which also implies that $\mathcal{G}$ is a Lyapunov function of the stochastic dynamics.

IV. MACROSCOPIC OR WEAK-NOISE LIMIT

We now consider that the system has a scale parameter $\Omega \equiv 1/\varepsilon$. We assume the following scaling:

$$\phi(\boldsymbol{x}) \equiv \lim_{\Omega \to \infty} \Phi(\boldsymbol{x})/\Omega \quad (23)$$

$$d_{nm}(\boldsymbol{x}) \equiv \Omega D_{nm}(\boldsymbol{x}) \quad (24)$$

$$u_n(\boldsymbol{x}) \equiv \lim_{\Omega \to \infty} \mu_n(\boldsymbol{x}) = -d_{nm}(\boldsymbol{x}) \partial_m \phi(\boldsymbol{x}) + f_n(\boldsymbol{x}). \quad (25)$$

As a result of the scalings [Eqs. (23)–(25)], for $\Omega \to \infty$, the solution $P(\boldsymbol{x})$ of the Fokker-Planck equation satisfies a large deviations principle

$$P(\boldsymbol{x}) \underset{\Omega \to \infty}{\asymp} e^{-\Omega I(\boldsymbol{x})} \,, \quad (26)$$

with the rate function $I(\boldsymbol{x}) = \lim_{\Omega \to \infty} \mathcal{I}(\boldsymbol{x})/\Omega$, which can be interpreted as the self-information density. Indeed, using Eqs. (7)–(9) with Eqs. (26) and (23)–(25), we find that for $\Omega \to \infty$, the rate function evolves according to

$$\partial_t I(\boldsymbol{x}) = -\partial_n I(\boldsymbol{x})\, u_n(\boldsymbol{x}) - \partial_n I(\boldsymbol{x})\, d_{nm}(\boldsymbol{x})\, \partial_m I(\boldsymbol{x}) \,. \quad (27)$$

The most probable state at a given time is the global minimum $\boldsymbol{x}_t$ of the instantaneous rate function $I(\boldsymbol{x})$. Multiplying both sides of the Fokker-Planck equation (3) by x and integrating over x, in the $\Omega \to \infty$ limit where the probability concentrates on $\boldsymbol{x}_t$, the latter is found to evolve according to the closed deterministic dynamics

$$d_t \boldsymbol{x}_t = \boldsymbol{u}(\boldsymbol{x}_t). \quad (28)$$

Proceeding in a similar manner, we now evaluate the first and second laws, as well as the adiabatic and/or nonadiabatic decomposition in the limit $\Omega \to \infty$. For any quantity $\langle A \rangle$, we consider its scaled version (or density) as $a(\boldsymbol{x}) \equiv \lim_{\Omega \to \infty} \langle A \rangle/\Omega$, and the same is done for the different thermodynamic quantities (e.g., $\langle \dot{Q} \rangle$, $\langle \dot{W} \rangle$, S, and $\mathcal{F}$). The first law, Eq. (10), reduces to:

$$d_t \phi(\boldsymbol{x}_t) = \dot{q}(\boldsymbol{x}_t) + \dot{w}(\boldsymbol{x}_t), \quad (29)$$

where

$$\dot{q}(\boldsymbol{x}) = -u_n(\boldsymbol{x})\, d^{-1}_{nm}(\boldsymbol{x})\, u_m(\boldsymbol{x}) \quad (30)$$

and

$$\dot{w}(\boldsymbol{x}) = u_n(\boldsymbol{x})\, d^{-1}_{nm}(\boldsymbol{x})\, f_m(\boldsymbol{x}) \quad (31)$$

are the scaled heat and work rates, respectively. The second law in Eq. (14) reduces to

$$\dot{\sigma}(\boldsymbol{x}_t) = -\dot{q}(\boldsymbol{x}_t) \geqslant 0. \quad (32)$$

Note that $d_t s \to 0$ for $\Omega \to \infty$, which is natural since, according to the large deviations principle, S scales as $\propto \ln \Omega$, so $s \to 0$ for $\Omega \to \infty$; there is no uncertainty regarding the microscopic state of the system in the absence of noise.

Evaluating the relative entropy $\mathcal{G}$ in the $\Omega \to \infty$ limit, we obtain

$$\lim_{\Omega\to\infty} \mathcal{G}/\Omega = I^{\rm ss}(\boldsymbol{x}_t), \tag{33}$$

where $I^{\rm ss}(\boldsymbol{x})$ is the steady-state rate function. Then, the scaled nonadiabatic entropy production rate, that is, the scaled version of Eq. (22), is

$$\dot\sigma_{\rm na} = -d_t I^{\rm ss}(\boldsymbol{x}_t), \tag{34}$$

and the fact that it is positive proves that $I^{\rm ss}(\boldsymbol{x})$ is a Lyapunov function of the deterministic dynamics. The positivity of the adiabatic entropy production rate implies that

$$d_t I^{\rm ss}(\boldsymbol{x}_t) + \dot\sigma(\boldsymbol{x}_t) \geqslant 0, \tag{35}$$

which is the emergent second law identified in [17] for Markov jump processes. Equation (35) is useful because it allows one to bound changes in steady-state self-information in terms of the entropy produced along deterministic dynamics, as we exemplify in Sec. VIII. A different and early derivation of this result, which apparently went unnoticed at the time, was presented by Gaveau and colleagues [27].

V. NONEQUILIBRIUM EXPANSION

We now consider the expansion of the steady-state rate function $I^{\rm ss}(\boldsymbol{x})$ in different powers of the force $f_n(\boldsymbol{x})$. We first split the drift $u_n(\boldsymbol{x})$ into zero- and first-order contributions:

$$u_n(\boldsymbol{x}) = \underbrace{-d_{nm}(\boldsymbol{x})\partial_m\phi(\boldsymbol{x})}_{u_n^{(0)}(\boldsymbol{x})} + \underbrace{f_n(\boldsymbol{x})}_{u_n^{(1)}(\boldsymbol{x})}. \tag{36}$$

We also split the steady-state rate function in a similar way:

$$I^{\rm ss}(\boldsymbol{x}) = I^{(0)}(\boldsymbol{x}) + I^{(1)}(\boldsymbol{x}) + I^{(2)}(\boldsymbol{x}) + \cdots \tag{37}$$

Substituting Eqs. (36) and (37) into Eq. (27), at steady state, we find to the lowest order

$$0 = -u_n^{(0)}(\boldsymbol{x}) - d_{nm}(\boldsymbol{x})\partial_m I^{(0)}(\boldsymbol{x}) \tag{38}$$

and for $k \geqslant 1$,

$$0 = -\partial_n I^{(k)}(\boldsymbol{x})\, u_n^{(0)}(\boldsymbol{x}) - \partial_n I^{(k-1)}(\boldsymbol{x})\, u_n^{(1)}(\boldsymbol{x}) - \sum_{j=0}^{k} \partial_n I^{(j)}(\boldsymbol{x})\, d_{nm}(\boldsymbol{x})\, \partial_m I^{(k-j)}(\boldsymbol{x}). \tag{39}$$

Equation (38) with Eq. (36) implies that $I^{(0)}(\boldsymbol{x}) = \phi(\boldsymbol{x})$ as expected. Equation (39), with Eqs. (36) and (38), can be rewritten as

$$u_n^{(0)}(\boldsymbol{x})\, \partial_n I^{(k)}(\boldsymbol{x}) = \partial_n I^{(k-1)}(\boldsymbol{x})\, f_n(\boldsymbol{x}) + \sum_{j=1}^{k-1} \partial_n I^{(j)}(\boldsymbol{x})\, d_{nm}(\boldsymbol{x})\, \partial_m I^{(k-j)}(\boldsymbol{x}). \tag{40}$$

An important feature of this equation is that it allows one to recursively solve for $I^{(k)}(\boldsymbol{x})$. We also note that $u_n^{(0)}(\boldsymbol{x}_t^{(0)})\, \partial_n I^{(k)}(\boldsymbol{x}_t^{(0)}) = d_t I^{(k)}(\boldsymbol{x}_t^{(0)})$, where $\boldsymbol{x}_t^{(0)}$ is a trajectory solving the zeroth-order deterministic dynamics $d_t \boldsymbol{x}_t^{(0)} = \boldsymbol{u}^{(0)}(\boldsymbol{x}_t^{(0)})$. In particular, the first-order component $I^{(1)}(\boldsymbol{x})$ satisfies

$$\begin{aligned} d_t I^{(1)}\big(\boldsymbol{x}_t^{(0)}\big) &= \partial_n\phi\big(\boldsymbol{x}_t^{(0)}\big)\, f_n\big(\boldsymbol{x}_t^{(0)}\big) \\ &= -u_m^{(0)}\big(\boldsymbol{x}_t^{(0)}\big)\, d_{mn}^{-1}\big(\boldsymbol{x}_t^{(0)}\big)\, f_n\big(\boldsymbol{x}_t^{(0)}\big) \\ &= -\dot w^{(1)}\big(\boldsymbol{x}_t^{(0)}\big), \end{aligned} \tag{41}$$

where, in the last line, we have used Eq. (31), and $\dot w^{(1)}$ denotes the lowest-order contribution to $\dot w$. We now introduce the notation $a^{[k]} = \sum_{j=0}^{k} a^{(k)}$ for the partial reconstruction of any quantity a up to order k. The first law, Eq. (29), to the first order in the nonconservative force f_n reads: $d_t I^{(0)} = d_t\phi \simeq \dot q^{[1]} + \dot w^{(1)}$. Together with Eqs. (41) and (32), we find that

$$d_t I^{[1]}\big(\boldsymbol{x}_t^{(0)}\big) = \dot q^{[1]}\big(\boldsymbol{x}_t^{(0)}\big) = -\dot\sigma^{[1]}\big(\boldsymbol{x}_t^{(0)}\big). \tag{42}$$

By comparing the last equation with Eq. (35), we see that the emergent second law is saturated to the first order in the force $f_n(\boldsymbol{x})$ along zeroth-order trajectories. This result is formally analogous to what was obtained for Markov jump processes admitting a large size limit [17,28]. We notice that this expansion is conceptually different from a previous one proposed by Bouchet and colleagues [29] as it takes the detailed-balance dynamics as the reference state. As a result of this choice, the different orders can be calculated recursively only using the relaxation dynamics with no need to consider optimal fluctuating trajectories (see Sec. VII).

VI. ORTHOGONAL DECOMPOSITION

Now we explore the consequences of decomposing the drift $\mu_n(\boldsymbol{x})$ in terms of the gradient of the steady-state self-information $\mathcal{I}^{\rm ss}(\boldsymbol{x}) = -\ln(P^{\rm ss}(\boldsymbol{x}))$. From Eq. (9), we have [30]

$$\mu_n(\boldsymbol{x}) = -D_{nm}(\boldsymbol{x})\partial_m \mathcal{I}^{\rm ss}(\boldsymbol{x}) + j_n^{\rm ss}(\boldsymbol{x}), \tag{43}$$

where $j_n^{\rm ss}(\boldsymbol{x})$ is the probability velocity at steady state. By evaluating Eq. (7) at steady state, we find that the probability velocity must satisfy the relation

$$0 = \partial_n j_n^{\rm ss}(\boldsymbol{x}) - \partial_n \mathcal{I}^{\rm ss}(\boldsymbol{x}) j_n^{\rm ss}(\boldsymbol{x}) \tag{44}$$

at each order in Ω. We consider the following expansions for the probability velocity

$$j_n^{\rm ss}(\boldsymbol{x}) = v_n(\boldsymbol{x}) + h_n(\boldsymbol{x})/\Omega + O(1/\Omega^2), \tag{45}$$

where $v_n(\boldsymbol{x}) = \lim_{\Omega\to\infty} j_n^{\rm ss}(\boldsymbol{x})$ is the macroscopic probability velocity, and for the self-information

$$\mathcal{I}^{\rm ss}(\boldsymbol{x}) = \Omega I^{\rm ss}(\boldsymbol{x}) + K^{\rm ss}(\boldsymbol{x}) + O(1/\Omega). \tag{46}$$

Using these expansions in Eq. (43), we find at the leading order Ω^0, the drift decomposition

$$u_n(\boldsymbol{x}) = -d_{nm}(\boldsymbol{x})\partial_m I^{\rm ss}(\boldsymbol{x}) + v_n(\boldsymbol{x}). \tag{47}$$

Using the same expansions in Eq. (44), we obtain to order Ω,

$$v_n(\boldsymbol{x})\partial_n I^{\rm ss}(\boldsymbol{x}) = 0. \tag{48}$$

Equation (48) shows that v_n is orthogonal to the level sets of $I^{\rm ss}$. Thus, $v_n(\boldsymbol{x}) = a_{nm}(\boldsymbol{x})\partial_m I^{\rm ss}(\boldsymbol{x})$, where a_{nm} is an antisymmetric matrix [31]. Higher-order terms in the drift decomposition can be used to determine the subleading correction $K^{\rm ss}$ to the quasipotential (see Sec. IX).

Using Eq. (21), the macroscopic limit of the mean adiabatic entropy production rate is

$$\dot{\sigma}_{\rm a} \equiv \lim_{\Omega\to\infty} \frac{1}{\Omega}\dot{\Sigma}_{\rm a} = v_n d^{-1}_{nm} v_m \geqslant 0. \tag{49}$$

Moreover, let us write $I^{\rm ss} = \phi + \psi$, with ψ not necessarily small, and seek an equation for ψ. First, we note that, from Eqs. (47) and (25), $v_n = f_n + d_{nm}\partial_m\psi$. Then, we can rewrite Eq. (48) as

$$0 = \underbrace{f_n\partial_n\phi}_{-\dot{w}^{(1)}} + \underbrace{f_n\partial_n\psi + d_{nm}\partial_n\psi\,\partial_m\psi}_{v_n\partial_n\psi} + \underbrace{d_{nm}\partial_n\phi\partial_n\psi}_{-d_t\psi(\boldsymbol{x}_t^{(0)})}. \tag{50}$$

With the orthogonality condition $0 = v_n\partial_n I^{\rm ss} = v_n\partial_n\phi + v_n\partial_n\psi$, we arrive at

$$d_t\psi\left(\boldsymbol{x}_t^{(0)}\right) = -\dot{w}^{(1)} - v_n\partial_n\phi. \tag{51}$$

This shows that the linear response approximation in Eq. (41) will work well when $v_n\partial_n\phi$ is small, that is, when the macroscopic velocity current lies on a level hypersurface of the potential ϕ.

VII. THERMODYNAMICS OF RARE TRAJECTORIES

We consider the overdamped Langevin equation corresponding to the Fokker-Planck equation (3),

$$d_t x_n = \mu_n(\boldsymbol{x}) + \sqrt{2}B_{nm}(\boldsymbol{x})\,\eta_m(t), \tag{52}$$

where the noise is Gaussian, zero-mean, and white,

$$\langle\eta_n(t)\rangle = 0, \quad \langle\eta_n(t)\eta_m(t')\rangle = \delta_{nm}\delta(t-t'), \tag{53}$$

and $B_{nk}(\boldsymbol{x})B_{mk}(\boldsymbol{x}) = D_{nm}(\boldsymbol{x})$. Since the noise in Eq. (52) is multiplicative, one should choose the anti-Ito (or "post-point" [32]) prescription to obtain the Fokker-Planck equation in Eq. (3). Along this same line, whenever we deal with products of fluctuating quantities throughout this paper, we consider the Stratonovich convention [33], without using any specific notation. However, all prescriptions are equivalent when we consider the leading order of the weak-noise limit.

The asymptotic limit $\Omega\to\infty$ reduces Eq. (52) to the deterministic expression already introduced in Eq. (28). We define the fixed points $\{\boldsymbol{x}^*\}$ of the deterministic dynamics as the solutions of the equations

$$u_n(\boldsymbol{x}^*) = 0. \tag{54}$$

Their stability can be inferred by studying the linearized dynamics in their vicinity [34],

$$d_t\delta x_n = \delta x_m\partial_m u_n(\boldsymbol{x}^*), \tag{55}$$

where $\delta\boldsymbol{x} \equiv \boldsymbol{x} - \boldsymbol{x}^*$. If all eigenvalues of the Jacobian matrix with elements $\partial_m u_n(\boldsymbol{x}^*)$ have the same (positive or negative) sign, $\boldsymbol{x}^*$ is called a (unstable or stable, respectively) node. Otherwise, it is called a saddle. If there are two stable fixed points $\boldsymbol{x}^*_{(i)}, \boldsymbol{x}^*_{(j)}$ separated by a saddle $\boldsymbol{x}^*_{(\nu)}$, we say that the system is bistable. When a small noise is added, the system displays metastability [6]. Note that non-detailed-balance dynamics admits more general attractors than fixed points, such as limit cycles, which are not considered in the following.

The metastable state is defined as the basin of attraction of a stable fixed point, namely the set of points that, if taken as the initial conditions for the noiseless dynamics of Eq. (28), would relax to the chosen fixed point [35]. In the framework of weak noise, a transition between states corresponds to an escape trajectory that, starting in the fixed point $\boldsymbol{x}^*_{(i)}$, after an ideally infinite time, reaches the saddle point $\boldsymbol{x}^*_{(\nu)}$ at the boundary with the basin of attraction of $\boldsymbol{x}^*_{(j)}$, that is,

$$\boldsymbol{x}(t=0) = \boldsymbol{x}^*_{(i)}, \quad \boldsymbol{x}(t\to\infty) = \boldsymbol{x}^*_{(\nu)}. \tag{56}$$

Once on the saddle, the trajectory follows a deterministic relaxation toward the target fixed point $\boldsymbol{x}^*_{(j)}$.

In the next paragraph, we show how the problem of calculating transition rates between metastable states in systems lacking detailed-balance relates to the search for the most likely escape trajectories. Knowledge of this trajectory will lead to the derivation of a thermodynamic upper bound on the nonequilibrium transition rate.

A. Optimal escape trajectory: The instanton

Considering the weak-noise limit, the dynamics for the rate function in Eq. (27) can be rewritten as a Hamilton-Jacobi equation:

$$-\partial_t I(x) = H(\boldsymbol{x}, \boldsymbol{\pi} = \nabla I(x)), \tag{57}$$

in terms of the Hamiltonian

$$H(\boldsymbol{x}, \boldsymbol{\pi}) = \boldsymbol{\pi}\cdot\boldsymbol{u}(\boldsymbol{x}) + \boldsymbol{\pi}^T\cdot\boldsymbol{d}(\boldsymbol{x})\cdot\boldsymbol{\pi}, \tag{58}$$

where $\boldsymbol{d}(\boldsymbol{x})$ is the scaled diffusion matrix. In Eq. (57), the rate function acts as the action function and $\boldsymbol{\pi} = \nabla I(x)$ as the conjugate momentum.

The equations of motion corresponding to such a Hamiltonian are:

$$d_t x_n = u_n(\boldsymbol{x}) + 2\,d_{nm}(\boldsymbol{x})\pi_m(\boldsymbol{x}) \tag{59}$$

$$d_t\pi_n = -\pi_k\,\partial_n u_k(\boldsymbol{x}) - \pi_j\,\partial_n d_{jk}(\boldsymbol{x})\,\pi_k. \tag{60}$$

These equations can be alternatively derived from a different perspective if the system is studied via the path integral approach. In fact, one can investigate the stochastic dynamics by looking at the path probability $P[\boldsymbol{x}]$ associated with the ensemble of trajectories $\{\boldsymbol{x}(t)\}_0^\tau$, constrained to the initial $\boldsymbol{x}(0)$ and final $\boldsymbol{x}(t)$, which is a generalization of the original Onsager-Machlup path probability to nonlinear systems [36]. In the asymptotic limit, we write

$$P[\boldsymbol{x}] \asymp \exp\left(-\Omega\int_0^t d\tau\,\frac{(\dot{\boldsymbol{x}}-\boldsymbol{u}(\boldsymbol{x}))\boldsymbol{d}(\boldsymbol{x})^{-1}(\dot{\boldsymbol{x}}-\boldsymbol{u}(\boldsymbol{x}))}{4}\right)$$
$$\equiv \exp(-\Omega\mathcal{A}[\boldsymbol{x},\dot{\boldsymbol{x}}]). \tag{61}$$

Using a Hubbard-Stratonovich transformation, we can rewrite it in Hamiltonian form:

$$P[\boldsymbol{x}] \asymp \int \mathcal{D}\boldsymbol{\pi}\, e^{-\Omega\int_0^t d\tau\,(\dot{\boldsymbol{x}}\cdot\boldsymbol{\pi} - H(\boldsymbol{x},\boldsymbol{\pi}))}. \tag{62}$$

Then, Eq. (59) is obtained by functional minimization of the action $\mathcal{A}$.

The system admits two classes of solutions that maximize the path probability (as we see in Fig. 8): solutions on the manifold $\boldsymbol{\pi} = 0$, corresponding to relaxation trajectories that, in fact, reduce Eq. (59) to $\dot{\boldsymbol{x}} = \boldsymbol{u}(\boldsymbol{x})$; and solutions with $\boldsymbol{\pi} \neq 0$, corresponding to the most typical path of large fluctuations, called instantons.

In particular, we observe that, when stationarity is reached for $t \to \infty$ in Eq. (57), we are left with $H(\boldsymbol{x}, \nabla I^{\rm ss}(\boldsymbol{x})) = 0$, which allows us to identify $\boldsymbol{\pi} = \nabla I^{\rm ss}$. Namely, the instanton solution must be found in the $H = 0$ manifold. The result is the infinite-time trajectory that, at the boundaries, satisfies Eq. (56).

At this point, the interest is on the derivation of the explicit equation of motion of the instanton. Replacing $\boldsymbol{\pi} = \nabla I^{\rm ss}$ in Eq. (59), we obtain:

$$\begin{aligned} d_t x_n &= u_n(\boldsymbol{x}) + 2\, d_{nm}(\boldsymbol{x}) \partial_m I^{\rm ss}(\boldsymbol{x}) \\ &= v_n(\boldsymbol{x}) + d_{nm}(\boldsymbol{x}) \partial_m I^{\rm ss}(\boldsymbol{x}), \end{aligned} \tag{63}$$

where in the second line, we employ the orthogonal decomposition of Eq. (47). Notice that, for the relaxation dynamics, we would have the opposite sign for the gradient of the quasipotential while the velocity term would be the same, as it is due to the current term, which characterizes the stationary state. Then, depending on the boundary conditions, the most likely velocity is

$$d_t x_n = v_n(\boldsymbol{x}) \pm d_{nm}(\boldsymbol{x}) \partial_m I^{\rm ss}(\boldsymbol{x}) \begin{cases} + & \text{if instanton} \\ - & \text{if relaxation.} \end{cases} \tag{64}$$

The previous equation shows how the presence of currents in a non-detailed-balance system breaks the symmetry between the relaxation and escape dynamics, which is retrieved for the case of zero nonconservative force $f = 0$, where the instanton becomes the time-reversed relaxation trajectory.

B. Bounding the transition rate

The exit time from a metastable state is known to obey an exponential law governed by a constant rate in the context of weak noise [10,37]. The rate can be obtained using the condition $H = 0$ in Eq. (62), in the infinite time limit for the instanton. Indeed, we have:

$$\begin{aligned} \lim_{t\to\infty} P[\boldsymbol{x}|\boldsymbol{x}(0) = \boldsymbol{x}^*_{(i)}, \boldsymbol{x}(t) = \boldsymbol{x}^*_{(\nu)}] \\ \asymp \exp\left(-\Omega \int d\tau\, \dot{\boldsymbol{x}} \cdot \nabla I^{\rm ss}(\boldsymbol{x}(t)) \Big|_{\boldsymbol{x}^*_{(i)}}^{\boldsymbol{x}^*_{(\nu)}} \right) \\ = e^{-\Omega (I^{\rm ss}(\boldsymbol{x}^*_{(\nu)}) - I^{\rm ss}(\boldsymbol{x}^*_{(i)}))}, \end{aligned} \tag{65}$$

which allows one to write

$$r_\nu \asymp e^{-\Omega (I^{\rm ss}(\boldsymbol{x}^*_{(\nu)}) - I^{\rm ss}(\boldsymbol{x}^*_{(i)}))}, \tag{66}$$

in full analogy to Arrhenius's formula for detailed-balance dynamics, where the quasipotential is just the equilibrium potential, that is, $I^{\rm ss} = \Phi$. Equation (66) can be shown to be controlled by lower and upper bounds of a thermodynamic nature.

To derive such thermodynamic bounds, the starting point is the general splitting of the fluctuating entropy flow in the environment into its housekeeping and excess parts [22,38]. The corresponding splitting of the total entropy production into adiabatic and nonadiabatic parts [26] would be recovered by adding the variation of the self-information (8), which is however superfluous, as it plays no role in the following derivation.

The entropy flow along a trajectory $\boldsymbol{x}(t)$ is given by the log-ratio of forward and backward path probabilities conditioned on their respective initial states, respectively denoted $P[\boldsymbol{x}]$ and $P[\overline{\boldsymbol{x}}]$ [18]:

$$\Sigma = \ln \frac{P[\boldsymbol{x}]}{P[\overline{\boldsymbol{x}}]}. \tag{67}$$

Defining the scaled functional $\sigma \equiv \lim_{\Omega\to\infty} \Sigma/\Omega$ and using Eq. (61) in Eq. (67), we obtain the explicit expression for the entropy flow along a trajectory of duration t,

$$\sigma = \int_0^t d\tau\, u_n(\boldsymbol{x})\, d^{-1}_{nm}(\boldsymbol{x})\, \dot{x}_m, \tag{68}$$

where $\dot{x}_m$ is given by Eq. (64). Recalling the decomposition of the scaled drift term in Eq. (47), we write the integrand in Eq. (68) as

$$(-d_{nm}(\boldsymbol{x}) \partial_m I^{\rm ss}(\boldsymbol{x}) + v_n)\, d^{-1}_{nm}(\boldsymbol{x})\, \dot{x}_m, \tag{69}$$

and expanding this product, we naturally identify two terms,

$$\sigma = -\int_0^t d\tau\, \partial_m I^{\rm ss}(\boldsymbol{x})\, \dot{x}_m + \int_0^t d\tau\, v_n(\boldsymbol{x})\, d^{-1}_{nm}(\boldsymbol{x})\, \dot{x}_m. \tag{70}$$

The first term in Eq. (70),

$$-\int_0^t \partial_m I^{\rm ss}(\boldsymbol{x})\, \dot{x}_m = I^{\rm ss}(\boldsymbol{x}_0) - I^{\rm ss}(\boldsymbol{x}_t) \equiv \sigma_{\rm na}, \tag{71}$$

is the macroscopic limit of the nonadiabatic entropy production. Its rate reduces to the nonadiabatic contribution [Eq. (34)] used in the emergent second law in Eq. (35) once it is evaluated along the deterministic relaxation trajectory. For the second contribution in Eq. (70), using the orthogonality condition [Eq. (48)], we can write

$$\int_0^t d\tau\, v_n(\boldsymbol{x})\, d^{-1}_{nm}(\boldsymbol{x})\, \dot{x}_m = \int_0^t d\tau\, v_n(\boldsymbol{x})\, d^{-1}_{nm}(\boldsymbol{x}) v_m(\boldsymbol{x}) \equiv \sigma_{\rm a} \geqslant 0, \tag{72}$$

which is the macroscopic limit of the adiabatic entropy production. It extends the result valid for the relaxation dynamics of Eq. (49) to the instanton trajectory.

The fact that Eq. (72) is non-negative irrespective of the dynamics considered, be they relaxational or instantonic, allows one to derive thermodynamic bounds on the transition rate of Eq. (66). Indeed, the nonadiabatic entropy production of the relaxation $\sigma_{\rm na}^{\nu\to i}$ is equal and opposite to the nonadiabatic entropy production of the instanton $\sigma_{\rm na}^{i\to\nu}$, being the difference between initial and final values of the quasipotential

$$\sigma_{\rm na}^{\nu\to i} = \Delta I^{\rm ss} = -\sigma_{\rm na}^{i\to\nu}. \tag{73}$$

Hereafter, $i \to \nu$ and $\nu \to i$ denote the instanton and relaxation trajectories, respectively, connecting the saddle ν with the stable fixed point i.

As a consequence, the following two inequalities hold:

$$\sigma_{i\to\nu} = \sigma_{\rm a}^{i\to\nu} - \Delta I^{\rm ss} \geqslant -\Delta I^{\rm ss}, \tag{74}$$

$$\sigma_{\nu\to i} = \sigma_{\rm a}^{\nu\to i} + \Delta I^{\rm ss} \geqslant \Delta I^{\rm ss}, \tag{75}$$

which are equivalent to

$$e^{\Omega\,\sigma_{i\to\nu}} \geqslant e^{-\Omega\,\Delta I^{\rm ss}}, \tag{76}$$

$$e^{-\Omega\,\sigma_{\nu\to i}} \leqslant e^{-\Omega\,\Delta I^{\rm ss}}. \tag{77}$$

The right-hand side of both inequalities corresponds to the leading order of the nonequilibrium transition rate appearing in Eq. (66), yielding the thermodynamic bounds on the transition rate

$$-\sigma_{\nu\to i} \leqslant \lim_{\Omega\to\infty} \frac{1}{\Omega} \ln r_\nu \leqslant \sigma_{i\to\nu}. \tag{78}$$

VIII. EXAMPLE

In this section, we illustrate our results by looking at the specific example of the two-dimensional double-well subjected to a rotational flow, which breaks detailed balance. First, in Sec. VIII A, we specify the model characteristics and study its deterministic dynamics. Then, in Sec. VIII B, we exemplify the use of the emergent second law, exploiting the fact that we can use entropy production as an upper bound for the steady state rate function $I^{\rm ss}$. To do so, we rely on an empirical estimate of such function $I^{\rm ss}_{\rm est}$. This estimate is obtained by deriving a histogram of the steady-state distribution along a reaction coordinate, as we explain in the second paragraph of this section. After that, in Sec. VIII C, we make use of the nonequilibrium expansion of the quasipotential in Eq. (40), evaluated up to the first and second orders in the shear, to show that there is good agreement compared with the aforementioned $I^{\rm ss}_{\rm est}$. Finally, in Sec. VIII D, we test the thermodynamic bounds of Eq. (78), after dealing with the problem of obtaining the instanton trajectory, which requires a sophisticated numerical technique.

A. The double well with shear flow

Our two-dimensional model is described by the following Langevin dynamics

$$\begin{aligned} d_t x_1 &= \mu_1(\boldsymbol{x}) + \sqrt{2/\Omega}\,\eta_1(t), \\ d_t x_2 &= \mu_2(\boldsymbol{x}) + \sqrt{2/\Omega}\,\eta_2(t), \end{aligned} \tag{79}$$

where $\eta_i(t)$ are zero-mean Gaussian variables satisfying Eq. (53). This corresponds to taking $D_{nm}(\boldsymbol{x}) = \Omega^{-1}\mathbb{I}_{2\times 2}$ in Eq. (4). For the drift, we consider the combination of a conservative force coming from a bistable potential and a nonconservative rotational field

$$\mu_n(\boldsymbol{x}) = -\Omega^{-1}\partial_n \Phi(\boldsymbol{x}) + f_n(\boldsymbol{x}), \tag{80}$$

where the potential $\Phi(\boldsymbol{x})$ is given by

$$\Phi(\boldsymbol{x}) = \Omega\big(\alpha x_1^4 - \beta x_1^2 + x_2^2\big), \tag{81}$$

and the force $f_n(\boldsymbol{x})$, corresponding to a shear flow, reads

$$f_1(\boldsymbol{x}) = -\gamma x_2 \quad f_2(\boldsymbol{x}) = \gamma x_1. \tag{82}$$

The constants α, β, and γ are free parameters. Figure 1 shows the equipotential lines of $\Phi(\boldsymbol{x})/\Omega$ and the direction of the force $\boldsymbol{f}(\boldsymbol{x})$. In Fig. 2, we show the steady-state distributions for different strengths of the force $\boldsymbol{f}(\boldsymbol{x})$ that were obtained from stochastic trajectories generated by the direct numerical integration of Eq. (79).

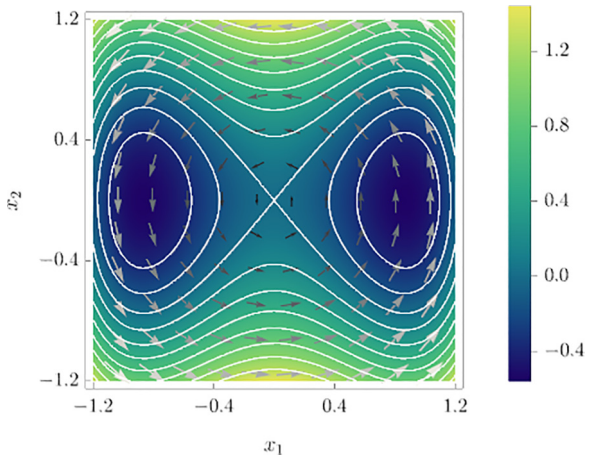

FIG. 1. Equipotential lines of $\Phi(\boldsymbol{x})/\Omega$. Arrows indicate the direction of the rotational field $\boldsymbol{f}(\boldsymbol{x})$. The parameters are $\alpha = 1$, $\beta = 1.5$, and $\gamma = 1$.

Before dealing with the emergent second law, it is useful to study the model deterministic dynamics $d_t\boldsymbol{x} = \boldsymbol{u}(\boldsymbol{x})$. It has three fixed points, $\boldsymbol{x}^* = 0$, and

$$x_1^* = \pm\tfrac{1}{2}\sqrt{(4\beta - \gamma^2)/2\alpha}, \quad x_2^* = \gamma\, x_1^*/2, \tag{83}$$

for $\gamma^2 < 4\beta$, while it has only one fixed point, $\boldsymbol{x}^* = 0$, for $\gamma^2 \geqslant 4\beta$. A linear stability analysis shows that $\boldsymbol{x}^* = 0$ is a stable fixed point only if $\gamma^2 > 4\beta$, while the other two fixed points are stable otherwise. An estimation based on a Gaussian approximation shows that the dominant effect of noise in the deterministic equations of motion (tracking the evolution of the mean values $\langle x_1\rangle$) is to renormalize the constant β as $\beta - 6\alpha\sigma_1^2$, where σ_1^2 is the variance of x_1, which decreases as $1/\Omega$ for large Ω. This can be obtained customarily by writing $\boldsymbol{x} = \langle\boldsymbol{x}\rangle + \delta\boldsymbol{x}$, expanding Eq. (79) to the second order in the fluctuations $\delta\boldsymbol{x}$, and averaging [18].

B. Emergent second law

According to the emergent second law in Eq. (35), given a trajectory $\boldsymbol{x}_t$ starting at a point $\boldsymbol{x}_0$, the macroscopic entropy production $\sigma(\boldsymbol{x}_0) = \int_0^{+\infty} d\tau\dot{\sigma}(\boldsymbol{x}_\tau)$ is an upper bound to $I^{\rm ss}(\boldsymbol{x_0})$, the steady-state rate function evaluated at the initial state of this nonequilibrium relaxation trajectory. This is useful since the steady-state rate function is usually hard to obtain while $\sigma(\boldsymbol{x}_0)$ can be computed from the deterministic dynamics alone. We implement this idea for points along the axis q joining the origin $x_1 = x_2 = 0$ with one deterministic fixed point $\boldsymbol{x}^*$. An example is shown in Fig. 2. In the first place, in Fig. 3 we show the histogram of the steady-state distribution for different values of q and $|p| < \epsilon = 10^{-2}$, where p is the coordinate orthogonal to q. From such a histogram, it is possible to obtain an estimate of the rate function as $I^{\rm ss}_{\rm est}(q) = -\ln(P(q\,|\,|p| < \epsilon))/\Omega$. Of course, for $I^{\rm ss}_{\rm est}(q)$ to be an accurate estimate of the true rate function, the value of Ω must be high enough, which makes the direct sampling of large fluctuations increasingly difficult. In Fig. 4 we compare the estimate $I^{\rm ss}_{\rm est}(q_0)$ (obtained from data generated with $\Omega = 30$), where q_0 is the starting point along reaction coordinate q, with the upper bound $\sigma(q_0)$. For $\gamma = 0$ we know that the

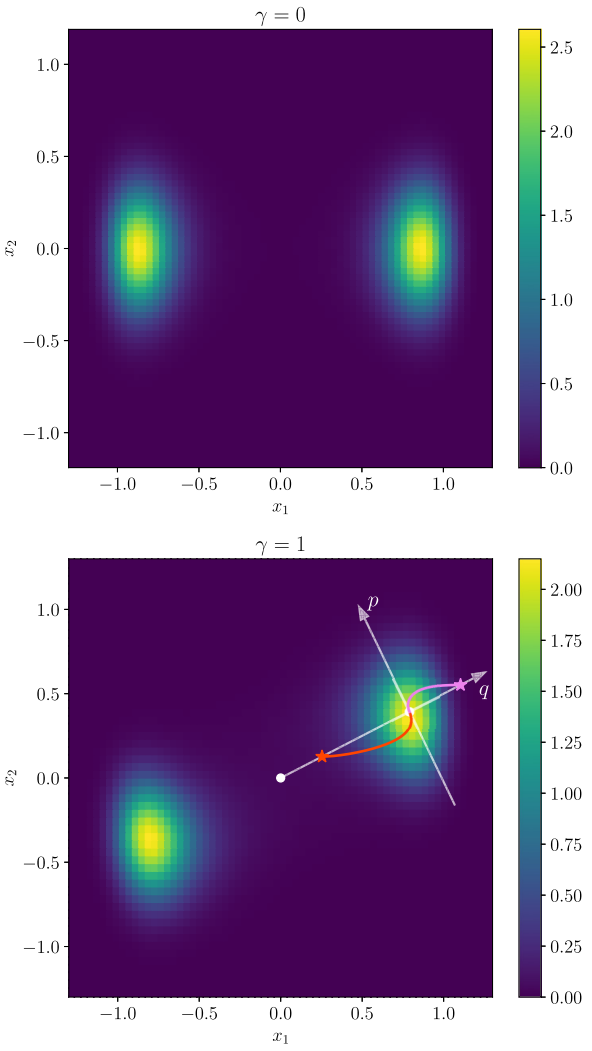

FIG. 2. Steady-state density histograms for different values of the force parameter γ. The top panel corresponds to $\gamma = 0$, and therefore shows the equilibrium distribution; the lower panel is for $\gamma = 1$. In the two cases, we have $\alpha = 1$, $\beta = 1.5$, and $\Omega = 10$. The data was obtained by numerical integration of Eq. (79). In the lower panel, we also show a new coordinate q (joining the origin and one deterministic fixed point $\boldsymbol{x}^*$) and two deterministic trajectories starting at different points (indicated by stars) and relaxing toward $\boldsymbol{x}^*$.

upper bound and the actual rate function coincide since the dynamics is detailed-balanced and the emergent second law is saturated in that case (indeed, the relaxation dynamics is actually the equilibrium one). We see in Fig. 4 that this is actually the case, which indicates that $\Omega = 30$ is already high enough to estimate the rate function. For $\gamma = 1$ we see that $\sigma(q_0)$ indeed works as an upper bound to $I^{\rm ss}_{\rm est}(q_0)$. The fact that the bound is tighter to the right of the fixed point can be traced back to the increased relaxation speed of the corresponding trajectories (see Ref. [17] for a detailed analysis of a similar observation).

C. Nonequilibrium expansion

We now illustrate the use of the nonequilibrium expansion in Sec. V. According to Eq. (40), contributions of different

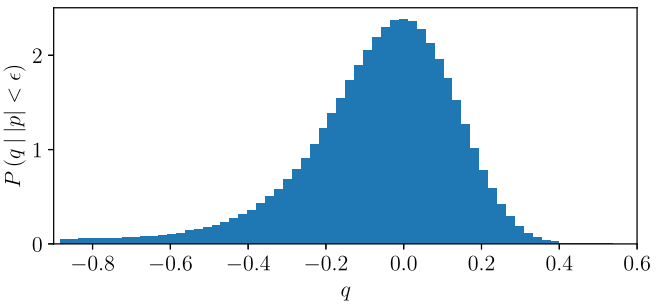

FIG. 3. Density histogram along the axis q in the lower panel of Fig. 2 ($\alpha = 1$, $\beta = 1.5$, $\gamma = 1$, $\Omega = 10$).

orders to the steady-sate rate function can be reconstructed by integrating different quantities over detailed-balanced deterministic trajectories, that is, those satisfying $d_t \boldsymbol{x}_t^{(0)} = \boldsymbol{u}^{(0)}(\boldsymbol{x}_t^{(0)})$. Examples of such trajectories are shown in Fig. 5. Note that they converge to the fixed point $\boldsymbol{x}^{*(0)}$ corresponding to $\gamma = 0$, in contrast to the deterministic trajectories involved in evaluating the emergent second law, which converge to the true fixed point for given parameters (Fig. 2).

In Fig. 6 we compare $I^{\rm ss}_{\rm est}(q_0)$, the numerical estimation of the rate function, with the first-order approximation $I^{[1]}(q_0)$ obtained by integrating Eq. (42). We see that the difference increases with γ, the strength of the rotational force field.

In principle, it is possible to compute the second-order correction to the rate function, which from Eq. (40) satisfies

$$u_n^{(0)}(\boldsymbol{x})\,\partial_n I^{(2)}(\boldsymbol{x}) = \partial_n I^{(1)}(\boldsymbol{x})\,f_n(\boldsymbol{x}) + \partial_n I^{(1)}(\boldsymbol{x})\,d_{nm}(\boldsymbol{x})\,\partial_m I^{(1)}(\boldsymbol{x}). \tag{84}$$

Therefore, to obtain $I^{(2)}(\boldsymbol{x})$ by integrating the previous equation along detailed-balanced deterministic trajectories, we must first compute the gradient of $I^{(1)}(\boldsymbol{x})$ at each point. Equation (40) gives directly the scalar product of such gradient and the velocity $\boldsymbol{u}^{(0)}(\boldsymbol{x})$, but we also need the other components. A possible strategy to obtain the full gradient of $I^{(1)}(\boldsymbol{x})$ is to compute it along sufficiently close trajectories. In our two-

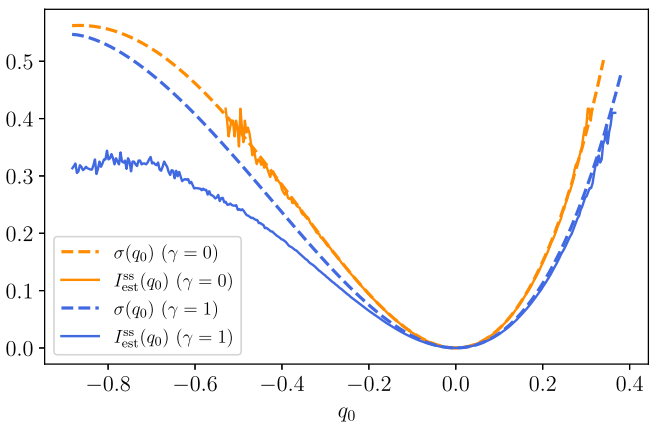

FIG. 4. Comparison between the estimation of the rate function $I^{\rm ss}_{\rm est}(q_0)$ and the integrated entropy production along deterministic trajectories $\sigma(q_0)$ as a function of q_0, the starting point along axis q. The parameters are $\alpha = 1$, $\beta = 1.5$, and $\Omega = 30$.

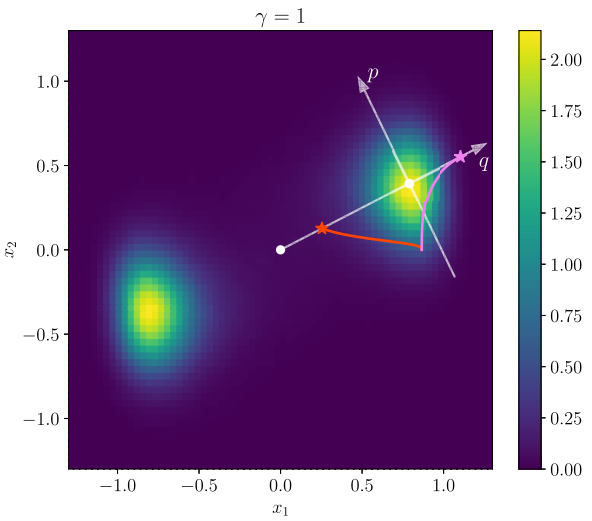

FIG. 5. Steady-state density histogram and two detailed-balanced deterministic trajectories starting at different points (indicated by stars) and relaxing toward $\boldsymbol{x}^{*(0)}$ [the fixed point of $d_t\boldsymbol{x}_t = \boldsymbol{u}^{(0)}(\boldsymbol{x}_t)$], for parameters $\alpha = 1$, $\beta = 1.5$, $\gamma = 1$, and $\Omega = 10$.

dimensional example, another option is to compute $I^{(1)}(\boldsymbol{x})$ for all points of a fine grid, as shown in Fig. 7. Then, it is possible to integrate Eq. (84) to obtain the second-order correction to the rate function. The final reconstruction of the rate function to that order is shown in Fig. 6 for two values of γ. It remains to be explored how to efficiently implement this procedure in high-dimensional systems.

D. Thermodynamic bounds

For the system defined by Eq. (79), we can derive deterministic relaxation and instanton trajectories. An example is

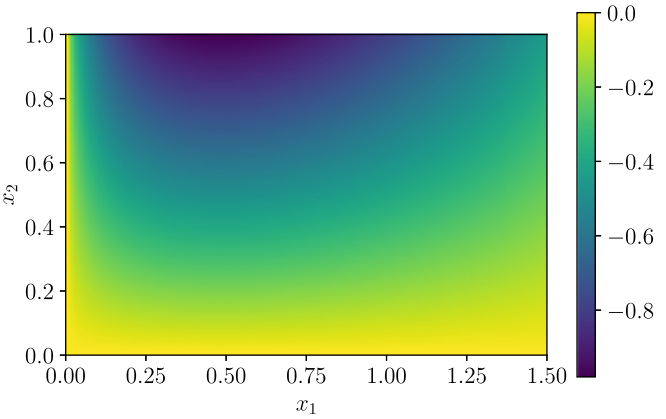

FIG. 7. First-order correction $I^{(1)}(\boldsymbol{x})$ computed by integrating Eq. (41) over trajectories starting at the points of a fine grid covering the region $0 \leqslant x_1 \leqslant 1.5$, $0 \leqslant x_2 \leqslant 1.0$ ($\alpha = 1$, $\beta = 1.5$, $\gamma = 1$).

reported in Fig. 8. By integrating along these trajectories, we can obtain upper and lower bounds on the transition rate r_v, following the procedure described in Sec. VII B. Figure 9 shows how the bounds [Eq. (78)] behave as the intensity of the shear changes through the quantity γ. A dedicated numerical method has been used to derive the three sets of points that appear in Fig. 9. First, the minimum action method (MAM) [39] has been implemented in Mathematica with the goal of deriving instantons—which is the main difficulty—for the chosen set of shear intensities γ. In principle, obtaining the instanton from equations Eqs. (59) and (60) is a boundary value problem that requires solving Eq. (63) with, for example, a shooting method. However, the MAM algorithm transforms the boundary value problem into an optimization problem. This is done by treating the physical time of the dynamics as an additional space coordinate, thus introducing an extra

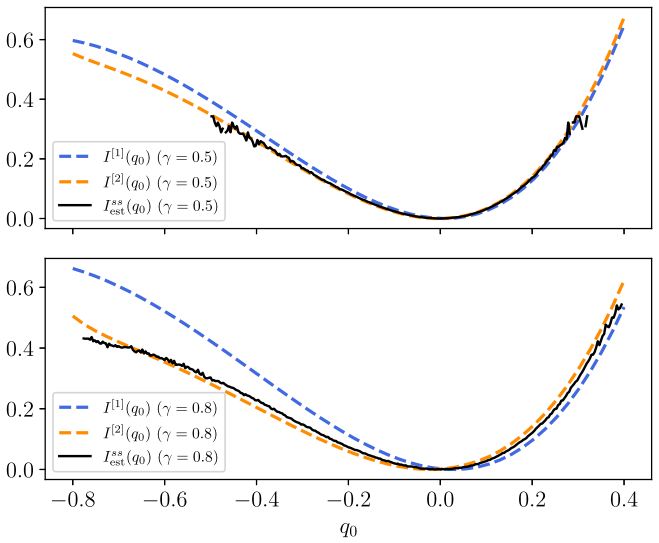

FIG. 6. Comparison between the estimation of the rate function $I^{ss}_{est}(q_0)$ with the first- and second-order approximations $I^{[1]}(q_0)$ and $I^{[2]}(q_0)$ obtained, respectively, from Eq. (42) and by considering also the contribution from Eq. (84). Simulations for two different values of γ ($\alpha = 1$, $\beta = 1.5$).

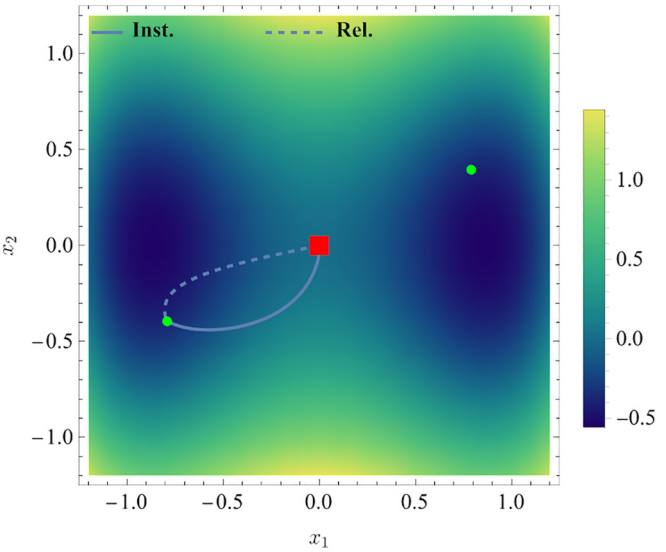

FIG. 8. Example of instanton (solid) and relaxation (dashed) trajectories for parameters $\alpha = 1$, $\beta = 1.5$, $\gamma = 1$, $\Omega = 30$. Green points represent the two symmetrical attractors, while the red square is the saddle point. Colormap represents the value of the potential $\Phi(\boldsymbol{x})/\Omega$ given in Eq. (81).

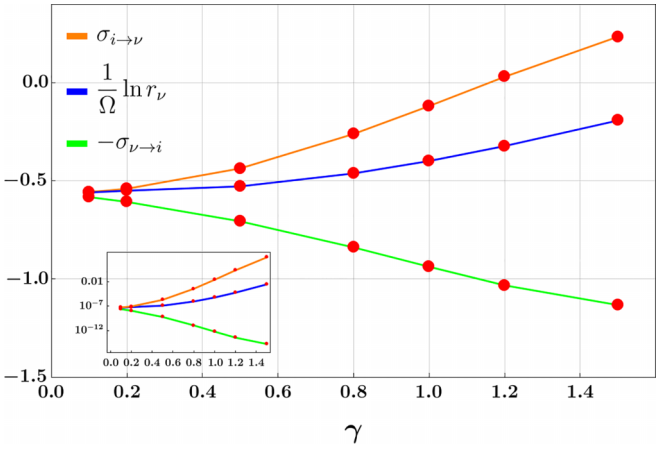

FIG. 9. Bounds for the nonequilibrium transition rate in Eq. (78) at different shear intensity. Data obtained with $\Omega = 30$. Inset: Quantities of the main plot multiplied by $\Omega = 30$ and exponentiated, representing in log-scale the bounds of Eqs. (76) and (77).

variable that plays the role of an artificial or algorithmic time τ. Within this framework, the method is an implementation of a gradient descend on the action $\mathcal{A}$, defined in Eq. (61), in the space of all possible trajectories allowed by the boundary conditions

$$\partial_\tau \hat{\boldsymbol{x}}(t,\tau) = -\frac{\delta \mathcal{A}}{\delta \hat{\boldsymbol{x}}}, \quad \hat{\boldsymbol{x}}(0,\tau) = \boldsymbol{x}^*, \quad \hat{\boldsymbol{x}}(t_f,\tau) = \boldsymbol{x}_\nu. \tag{85}$$

Having found the instanton as $\boldsymbol{x}(t) = \lim_{\tau\to\infty} \hat{\boldsymbol{x}}(t,\tau)$, one can numerically obtain the auxiliary momentum $\boldsymbol{\pi}(\boldsymbol{x})$ from Eq. (59), as the velocity can be numerically estimated *a posteriori*. We showed that the instanton is the trajectory for which $\boldsymbol{\pi} = \nabla I^{\rm ss}$, therefore the estimation of $\Delta I^{\rm ss}$ that defines the nonequilibrium transition rate according to Eq. (66) is completed by performing the integration $\Delta I^{\rm ss} = \int d\boldsymbol{x} \cdot \boldsymbol{\pi}(\boldsymbol{x})$ between the stable point $\boldsymbol{x}_i$ and the saddle $\boldsymbol{x}_\nu$. The upper bound in Eq. (78) is computed along the instanton, where the entropy rate is defined as $\dot\sigma = \boldsymbol{u}(\boldsymbol{x}) \cdot \dot{\boldsymbol{x}}$. The lower bound is instead computed by integrating the same quantity along the relaxation trajectory for each γ value, which is easily obtained via direct integration, as this dynamics given by a simpler initial value problem.

As $\gamma \to 0$, the bounds tend to saturate as expected. In that case, we retrieve equilibrium where $\sigma_{i\to\nu} = -\sigma_{\nu\to i}$ under time reversal, as expected from the odd nature of dissipation.

IX. SUBLEADING CORRECTION TO THE RATE FUNCTION

While the leading-order results of the previous sections only depend on the asymptotic scaling [Eq. (25)], the derivation of the subleading correction K to the rate function requires specifying the subleading behavior of the functions D_{nm}, Φ, and μ_n. Hereafter, we assume the homogeneous scaling

$$\Phi = \Omega\phi, \quad D_{nm} = d_{nm}/\Omega, \quad \mu_n = u_n. \tag{86}$$

This is a stronger assumption than the scaling in Eq. (25), which is instead the only condition required for the validity of all large-deviation results.

Using the expansions in Eqs. (45) and (46) in Eq. (43) together with the scaling in Eq. (86), we find the subleading order Ω^{-1} of the drift decomposition

$$h_n(\boldsymbol{x}) = d_{nm}(\boldsymbol{x})\partial_m K^{\rm ss}(\boldsymbol{x}). \tag{87}$$

Using the same expansions in Eq. (44), we obtain to subleading order Ω^0

$$\partial_n v_n(\boldsymbol{x}) - v_n(\boldsymbol{x})\partial_n K^{\rm ss}(\boldsymbol{x}) - h_n(\boldsymbol{x})\partial_n I^{\rm ss}(\boldsymbol{x}) = 0. \tag{88}$$

We can then leverage the instanton dynamics to obtain the subleading correction $K^{\rm ss}$ to the quasipotential $I^{\rm ss}$ in the stationary probability density

$$p^{\rm ss}(\boldsymbol{x}) = \exp\{-\Omega I^{\rm ss}(\boldsymbol{x}) - K^{\rm ss}(\boldsymbol{x}) + O(1/\Omega)\}. \tag{89}$$

From Eqs. (87) and (88), one gets

$$\partial_n v_n = (d_{mn}\partial_m I^{\rm ss} + v_n)\partial_n K^{\rm ss}. \tag{90}$$

Since the matrix d is symmetric, one verifies that

$$\begin{aligned}\partial_n v_n &= (d_{nm}\partial_m I^{\rm ss} + v_n)\partial_n K^{\rm ss} = d_t \boldsymbol{x}_{\rm ins} \cdot \partial_{\boldsymbol{x}} K^{\rm ss} \\ &= d_t K^{\rm ss}(\boldsymbol{x}_{\rm ins}(t)),\end{aligned} \tag{91}$$

where $\boldsymbol{x}_{\rm ins}(t)$ denotes the solution to the instanton dynamics in Eq. (63). The correction $K^{\rm ss}$ can therefore be obtained by integrating Eq. (91) along the instanton trajectory (see Sec. VII):

$$K^{\rm ss}(\boldsymbol{x}) - K^{\rm ss}(\boldsymbol{x}^*) = \int_0^\infty \partial_n v_n(\boldsymbol{x}_{\rm ins}(t))dt. \tag{92}$$

A similar formula was obtained by and [10] starting from the Langevin equation [Eq. (52)] interpreted according to Ito's calculus. The two results are identical in the case of additive noise, that is, when the matrix d is state-independent. Equation (92) shows that a solenoidal macroscopic probability velocity entails no correction to the rate function. Nonequilibrium probability distributions that are solely determined by the rate function are called Gibbs states [10]. Note that $-\partial_n v_n$ is the leading-order expression of the phase-space contraction rate as obtained by rewriting the Fokker-Planck equation, Eq. (7), in the form

$$\frac{d}{dt}\ln p = -\partial_n j_n \underset{t\to\infty}{=} -\partial_n v_n + O(1/\Omega), \tag{93}$$

where $d/dt = \partial_t + j_n\partial_n$ is the material derivative, that is, the total time derivative acting along trajectories with local mean velocity j_n. The long-time limit ensures that the system reaches stationarity, which allows one to replace j_n with the stationary velocity v_n at the leading order. The phase-space contraction rate plays a key role in the statistical mechanics of thermostated Hamiltonian systems [40,41], corresponding to the thermodynamic entropy production rate under special conditions [42].

It is also interesting to relax Eq. (86) and consider a thermodynamic potential of the type

$$\Phi(\boldsymbol{x}) = \Omega\phi(\boldsymbol{x}) + \varphi(\boldsymbol{x}) + O(\Omega^{-1}), \tag{94}$$

which complies with the scaling [Eq. (25)] necessary for the large deviations results on $I^{\rm ss}$. In this case,

$$\mu_n = u_n + w_n/\Omega + O(\Omega^{-2}), \tag{95}$$

with $w_n \equiv -d_{nm}\partial_m\varphi$, and Eq. (90) is replaced by

$$\begin{aligned}\partial_n v_n &= (d_{mn}\partial_m I^{\rm ss} + v_n)\partial_n K^{\rm ss} + w_n\partial_n I^{\rm ss} \\ &= d_t(K^{\rm ss} - \varphi)(\boldsymbol{x}_{\rm ins}(t)) + v_n\partial_n\varphi. \end{aligned} \tag{96}$$

For detailed-balanced dynamics, $v_n = 0$, so Eq. (96) correctly gives $K^{\rm ss} = \varphi + \text{const}$. In general, we obtain

$$K^{\rm ss}(\boldsymbol{x}) = \varphi(\boldsymbol{x}) + \int_0^\infty [\partial_n v_n - v_n\partial_n\varphi](\boldsymbol{x}_{\rm ins}(t))dt + \text{const}, \tag{97}$$

which reduces to Eq. (92) if $\varphi = 0$.

X. CONCLUSION

In this paper, we bridged Freidlin-Wentzell large deviations theory with nonequilibrium stochastic thermodynamics of isolated attractors within the context of non-detailed-balance systems described by overdamped diffusion. We succeeded in connecting the steady-state rate function, known as the quasipotential, to the energy and dissipation of the system. First, we derived a series expansions around the detailed-balance dynamics [Eq. (40)] that provides a powerful tool to numerically evaluate $I^{\rm ss}$ for nonequilibrium systems, given that it only makes use of the deterministic relaxation dynamics. This result suggests a straightforward iterative numerical procedure to obtain the quasipotential up to the nth order, as the relaxation dynamics can be easily implemented with well-established time-integration algorithms, which are fast and relatively inexpensive. How the method performs as the system dimension d or the magnitude of the nonconservative forces grows remains to be explored. Second, with the knowledge of the quasipotential, one can determine the escape rate r from an isolated attractor according to Eq. (66). We showed that quasipotential barriers are constrained by thermodynamics [see Eq. (78)]. Even though such expression consists of inequalities rather than strict equalities, this result is reminiscent of the Arrhenius law, given that the lifetime of the attractors is linked to the energy spent to relax into it, or escape from it. This expression also has the advantage of relying on an experimentally accessible quantity. Moreover, for weak forcing such that the gap between the lower and upper bounds is not wide, Eq. (78) becomes not just a physically relevant limit for the dynamics of the system but also a reliable predictive tool that allows us to derive a reasonable approximation of the escape rate.

ACKNOWLEDGMENTS

M.E. acknowledges financial support from project TheCirco (INTER/FNRS/20/15074473), funded by FRS-FNRS (Belgium) and FNR (Luxembourg). G.F. is funded by the European Union (NextGenerationEU) and by the program STARS@UNIPD with project "ThermoComplex."

[1] G. Margazoglou, T. Grafke, A. Laio, and V. Lucarini, Dynamical landscape and multistability of a climate model, Proc. R. Soc. A. **477**, 20210019 (2021).
[2] M. Assaf, E. Roberts, Z. Luthey-Schulten, and N. Goldenfeld, Extrinsic noise driven phenotype switching in a self-regulating gene, Phys. Rev. Lett. **111**, 058102 (2013).
[3] N. Freitas, K. Proesmans, and M. Esposito, Reliability and entropy production in nonequilibrium electronic memories, Phys. Rev. E **105**, 034107 (2022).
[4] H. Eyring, The activated complex in chemical reactions, J. Chem. Phys. **3**, 107 (1935).
[5] H. A. Kramers, Brownian motion in a field of force and the diffusion model of chemical reactions, Physica **7**, 284 (1940).
[6] S. Arrhenius, Über die reaktionsgeschwindigkeit bei der inversion von rohrzucker durch säuren, Z. Phys. Chem. **4U**, 226 (1889).
[7] P. Hänggi, P. Talkner, and M. Borkovec, Reaction-rate theory: Fifty years after Kramers, Rev. Mod. Phys. **62**, 251 (1990).
[8] M. I. Freidlin and A. D. Wentzell, *Random Perturbations of Dynamical Systems* (Springer, Berlin, Germany, 1998).
[9] F. Bouchet, J. Laurie, and O. Zaboronski, Langevin dynamics, large deviations and instantons for the quasi-geostrophic model and two-dimensional Euler equations, J. Stat. Phys. **156**, 1066 (2014).
[10] F. Bouchet and J. Reygner, Generalisation of the eyring–kramers transition rate formula to irreversible diffusion processes, Ann. Henri Poincaré **17**, 3499 (2016).
[11] H. Touchette, The large deviation approach to statistical mechanics, Phys. Rep. **478**, 1 (2009).
[12] R. Graham and T. Tél, Nonequilibrium potential for coexisting attractors, Phys. Rev. A **33**, 1322 (1986).
[13] R. Graham, Macroscopic potentials, bifurcations and noise in dissipative systems, in *Fluctuations and Stochastic Phenomena in Condensed Matter*, edited by L. Garrido, Lecture Notes in Physics, Vol. 268 (Springer, Berlin, Heidelberg, 1987), pp. 1–34.
[14] E. Weinan and E. Vanden-Eijnden, Minimum action method for the study of rare events, Commun. Pure Appl. Math. **57**, 637 (2004).
[15] T. Grafke, T. Schäfer, and E. Vanden-Eijnden, Long term effects of small random perturbations on dynamical systems: Theoretical and computational tools, in *Recent Progress and Modern Challenges in Applied Mathematics, Modeling and Computational Science*, edited by R. Melnik, R. Makarov, and J. Belair, Fields Institute Communications, Vol. 79 (Springer, New York, NY, 2017), pp. 17–55.
[16] F. Avanzini, M. Bilancioni, V. Cavina, S. Dal Cengio, M. Esposito, G. Falasco, D. Forastiere, J. N. Freitas, A. Garilli, P. E. Harunari *et al.*, Methods and conversations in (post) modern thermodynamics, SciPost Physics Lecture Notes **080**, (2024).
[17] J. N. Freitas and M. Esposito, Emergent second law for nonequilibrium steady states, Nat. Commun. **13**, 5084 (2022).
[18] G. Falasco and M. Esposito, Macroscopic stochastic thermodynamics, Rev. Mod. Phys. **97**, 015002 (2025).
[19] L. Bertini, A. De Sole, D. Gabrielli, G. Jona-Lasinio, and C. Landim, Macroscopic fluctuation theory, Rev. Mod. Phys. **87**, 593 (2015).

[20] P. Zhou and T. Li, Construction of the landscape for multi-stable systems: Potential landscape, quasi-potential, A-type integral and beyond, J. Chem. Phys. **144**, 094109 (2016).
[21] L. Peliti and S. Pigolotti, *Stochastic Thermodynamics: An Introduction* (Princeton University Press, 2021).
[22] U. Seifert, Stochastic thermodynamics, fluctuation theorems, and molecular machines, Rep. Prog. Phys. **75**, 126001 (2012).
[23] C. Van den Broeck and M. Esposito, Ensemble and trajectory thermodynamics: A brief introduction, Physica A **418**, 6 (2015).
[24] P. Gaspard, *The Statistical Mechanics of Irreversible Phenomena* (Cambridge University Press, 2022).
[25] N. Shiraishi, *An Introduction to Stochastic Thermodynamics* (Springer, 2023).
[26] C. Van den Broeck and M. Esposito, Three faces of the second law. II. Fokker-Planck formulation, Phys. Rev. E **82**, 011144 (2010).
[27] B. Gaveau, M. Moreau, and J. Toth, Dissipation of energy and of information in nonequilibrium reaction-diffusion systems, Phys. Rev. E **58**, 5351 (1998).
[28] N. Freitas, G. Falasco, and M. Esposito, Linear response in large deviations theory: A method to compute non-equilibrium distributions, New J. Phys. **23**, 093003 (2021).
[29] F. Bouchet, K. Gawredzki, and C. Nardini, Perturbative calculation of quasi-potential in non-equilibrium diffusions: A mean-field example, J. Stat. Phys **163**, 1157 (2016).
[30] H. Qian, Y.-C. Cheng, and Y.-J. Yang, Kinematic basis of emergent energetics of complex dynamics, Europhys. Lett. **131**, 50002 (2020).
[31] Y.-J. Yang and Y.-C. Cheng, Potentials of continuous markov processes and random perturbations, J. Phys. A: Math. Theor. **54**, 195001 (2021).
[32] S. Bo, S. H. Lim, and R. Eichhorn, Functionals in stochastic thermodynamics: how to interpret stochastic integrals, J. Stat. Mech. (2019) 084005.
[33] K. Sekimoto, *Stochastic Energetics*, Lecture Notes in Physics, Vol. 799 (Springer, 2010).
[34] S. H. Strogatz, *Nonlinear Dynamics and Chaos with Student Solutions Manual: With Applications to Physics, Biology, Chemistry, and Engineering* (CRC Press, 2018).
[35] G. Falasco and M. Esposito, Local detailed balance across scales: From diffusions to jump processes and beyond, Phys. Rev. E **103**, 042114 (2021).
[36] L. F. Cugliandolo and V. Lecomte, Rules of calculus in the path integral representation of white noise Langevin equations: The Onsager-Machlup approach, J. Phys. A: Math. Theor. **50**, 345001 (2017).
[37] M. V. Day, On the exponential exit law in the small parameter exit problem, Stochastics **8**, 297 (1983).
[38] T. Hatano and S.-I. Sasa, Steady-state thermodynamics of Langevin systems, Phys. Rev. Lett. **86**, 3463 (2001).
[39] R. Zakine and E. Vanden-Eijnden, Minimum-action method for nonequilibrium phase transitions, Phys. Rev. X **13**, 041044 (2023).
[40] D. J. Evans, Probability of second law violations in shearing steady states, Phys. Rev. Lett. **71**, 2401 (1993).
[41] G. Gallavotti and E. G. D. Cohen, Dynamical ensembles in nonequilibrium statistical mechanics, Phys. Rev. Lett. **74**, 2694 (1995).
[42] E. G. D. Cohen and L. Rondoni, Note on phase space contraction and entropy production in thermostatted Hamiltonian systems, Chaos **8**, 357 (1998).